Geophys. J. R. astr. Soc. (1971) **23**, 207–223.

The Analysis of Surface Wave Spectra Using a Reciprocity Theorem for Surface Waves

A. Douglas, J. A. Hudson and V. K. Kembhavi

(Received 1970 October 29)

Summary

By the use of a reciprocity theorem for surface waves, the mathematical expression for the spectrum of surface waves from a point source in a plane layered solid medium can be factorized into a component involving the transmission path and a component involving the source mechanism and depth. This second component can be easily constructed from expressions for the displacement and stress in a propagating surface wave.

The factorization has been used to study the effect of source mechanism and depth on the magnitude of the surface waves generated from point sources. In particular this study shows how holes may appear in the surface wave spectra due to the principle that it is impossible to excite a mode of oscillation by action at a node; it also throws doubt on the applicability of the depth correction terms currently used in the formula for M_s.

1. Introduction

In the course of a programme aimed at computing theoretical seismograms for teleseismic body and surface waves, it was noticed that in certain cases the spectrum of the Rayleigh waves appeared with a zero at a frequency which varied with depth and mechanism of the source and also with the azimuth of the observer. The origin of these zeros was tentatively attributed to the physical principle that one cannot excite a mode of oscillation of a system by striking it at a node of displacement.

In this paper we test this idea and show that it is correct. Zeros appear in Rayleigh wave and Love spectra according to the position of zeros of displacement or stress in the relevant surface wave. The theory is constructed on the basis of a reciprocity theorem for surface waves.

The elastodynamic reciprocal theorem for a bounded solid was given by Graffi (1947) and extended to unbounded media by Wheeler & Sternberg (1968). These theorems apply to the total displacement generated in the medium. In the Appendix we prove an equivalent theorem, applying to the far field surface wave displacements from body forces acting in a half-space whose properties vary with depth only.

2. Rayleigh waves from a double–couple source

We substitute into the reciprocal theorem for surface waves (equation (A22)) expressions giving the body forces and resulting displacements in two different systems of wave generation in a half space. The half space (defined by $z \geqslant 0$ with

respect to cylindrical polar co-ordinates r, ϕ, z) has a free upper surface and its elastic properties vary with the depth co-ordinate z only.

The first system is taken to be due to a double couple of magnitude $Q(t)$ at depth h below the origin of co-ordinates; its orientation is defined by unit vectors $\mathbf{f}$, $\mathbf{n}$ normal to the null planes. So the body force is

$$f_j^1 = -Q(t)(f_j n_k + f_k n_j) \frac{\partial}{\partial x_k} [\delta(x_1)\delta(x_2)\delta(x_3 - h)], \tag{2.1}$$

where the x_i are cartesian co-ordinates with $x_3 = z$ and x_1 along $\phi = 0$.

The second system is taken to be due to a vertical point force of unit magnitude acting at the surface at a large distance r_1 from the origin and at azimuth ϕ_1:

$$f_j^2 = \delta_{j3}\delta(x_1 - r_1 \cos\phi_1)\delta(x_2 - r_1 \sin\phi_1)\delta(x_3)\delta(t). \tag{2.2}$$

The reciprocal theorem (A22) gives

$$\bar{u}_z^{1q}(r_1, \phi_1, 0, \omega) = \bar{Q}(\omega)(f_j n_k + f_k n_j) \frac{\partial}{\partial x_k} \bar{u}_j^{2q}(0, \phi_1 + \pi, h, \omega)$$

$$= 2\bar{Q}(\omega)\, \bar{\varepsilon}_{fn}^{2q}(\phi_1 + \pi, h, \omega) \tag{2.3}$$

where the superscript q denotes the surface (in this case Rayleigh) wave and $\bar{\varepsilon}_{fn}^{2q}$ is the shear strain related to co-ordinates parallel to $\mathbf{f}$ and $\mathbf{n}$, at depth h below the origin, in the Rayleigh wave generated by the vertical point force at $(r_1, \phi_1, 0)$ and leaving the source at azimuth $\phi_1 + \pi$; the bar denotes the Fourier transform in time.

The waves generated by a vertical point force are independent of azimuth and the Rayleigh waves at large distances from any source are approximately plane and of a standard form (with horizontal and vertical components $u^R(z, \omega)$, $v^R(z, \omega)$ say). Hence we may write approximately in the neighbourhood of the origin,

$$\left.\begin{aligned} \bar{u}_1^{2q}(0, \phi_1 + \pi, z, \omega) &= -Cu^R(z, \omega)\cos\phi_1 \\ \bar{u}_2^{2q}(0, \phi_1 + \pi, z, \omega) &= -Cu^R(z, \omega)\sin\phi_1 \\ \bar{u}_3^{2q}(0, \phi_1 + \pi, z, \omega) &= Cv^R(z, \omega) \end{aligned}\right\} \tag{2.4}$$

where C is a constant and u^R, v^R contain a factor $\exp i\kappa(x_1 \cos\phi_1 + x_2 \sin\phi_1)$; κ is the Rayleigh wave number. The strain component $\bar{\varepsilon}_{fn}^{2q}$ becomes

$$\bar{\varepsilon}_{fn}^{2q} = \tfrac{1}{2}C\left[i\kappa(q_0 - q_2)\, u^R + i\kappa\, q_1 v^R + 2q_0 \frac{\partial v^R}{\partial z} - q_1 \frac{\partial u^R}{\partial z}\right], \tag{2.5}$$

where

$$\begin{aligned} q_0 &= f_3 n_3 \\ q_1 &= (f_1 n_3 + f_3 n_1)\cos\phi_1 + (f_2 n_3 + f_3 n_2)\sin\phi_1 \\ q_2 &= (f_1 n_1 - f_2 n_2)\cos 2\phi_1 + (f_1 n_2 + f_2 n_1)\sin 2\phi_1. \end{aligned}$$

Thus, dropping subscripts and superscripts 1, we get

$$\bar{u}_z^q(r, \phi, 0, \omega) = \bar{Q}(\omega)\, \bar{u}_z^{2q}(r, 0, \omega)\left[i\kappa(q_0 - q_2)\frac{u^R(h, \omega)}{v^R(0, \omega)}\right.$$

$$\left. + i\kappa q_1 \frac{v^R(h, \omega)}{v^R(0, \omega)} + \frac{2q_0}{v^R(0, \omega)}\left(\frac{\partial v^R}{\partial z}\right)_{z=h} - \frac{q_1}{v^R(0, \omega)}\left(\frac{\partial u^R}{\partial z}\right)_{z=h}\right] \tag{2.6}$$

corresponding to radiation as Rayleigh waves from the double-couple source, where $\bar{u}_z^{2q}(r, z, \omega)$ is the Rayleigh wave radiation from a unit vertical force acting on the surface at $r = 0$. I. N. Gupta (1966) has derived expressions such as (2.6) in a similar way (without any reference to the correct reciprocity theorem) but in rather less detail in order to calculate radiation patterns.

The effect on the Rayleigh wave spectrum of the fault mechanism and depth of focus is contained entirely in the factor in square brackets on the right-hand side of equation (2.6). Even if the transmission path is more complex than in the model we have used, so long as the complexities at a given azimuth involve merely a linear transformation on the expression for the radiation (i.e. multiplication of the spectrum by a transfer function), the effect of source mechanism and depth will still be described by the expression in square brackets. Two different sources in the neighbourhood of one another may be compared by comparing spectra at given azimuths.

Equation (2.6) therefore presents a possible method, by the use of Rayleigh wave spectra of checking fault-plane solutions and of fixing depth of focus fairly precisely, when the structure of the crust and upper mantle in the neighbourhood of the fault is known. Clearly this applies only to faults which are sufficiently small to be regarded as point sources.

Burridge, Lapwood & Knopoff (1964) have shown that the radiation from a point source of transverse slip (i.e. double couple) may be written as a linear combination of the responses to three basic sources, vertical dip slip, vertical strike slip and dip slip on a plane dipping at an angle of 45°. Therefore we shall examine these cases individually.

For vertical dip slip, $\mathbf{f} = (0, 0, 1)$, $\mathbf{n} = (0, 1, 0)$ and equation (2.6) becomes

$$\bar{u}_z^q(r, \phi, 0, \omega) = \bar{Q}(\omega)\,\bar{u}_z^{2q}(r, 0, \omega)\sin\phi\left[\frac{i\kappa v^R(h, \omega) - \left(\frac{\partial u^R}{\partial z}\right)_{z=h}}{v^R(0, \omega)}\right]$$

$$= -\bar{Q}(\omega)\,\bar{u}_z^{2q}(r, 0, \omega)\frac{\sin\phi}{\mu_m}\left(\frac{\tau^R(h, \omega)}{v^R(0, \omega)}\right), \qquad (2.7)$$

where τ^R is the shear stress on a horizontal plane in the Rayleigh wave, and μ_m is the rigidity at the source.

For a vertical strike slip, $\mathbf{f} = (1, 0, 0)$, $\mathbf{n} = (0, 1, 0)$ and

$$\bar{u}_z^q(r, \phi, 0, \omega) = -\bar{Q}(\omega)\,\bar{u}_z^{2q}(r, 0, \omega)\sin 2\phi\left[\frac{i\kappa u^R(h, \omega)}{v^R(0, \omega)}\right]. \qquad (2.8)$$

For dip slip on a plane inclined at 45° to the horizontal we may take

$$\mathbf{f} = (0, 1/\sqrt{2}, -1/\sqrt{2}), \qquad \mathbf{n} = (0, 1/\sqrt{2}, 1/\sqrt{2})$$

and then

$$\bar{u}_z^q(r, \phi, 0, \omega) = -\bar{Q}(\omega)\,\bar{u}_z^{2q}(r, 0, \omega)\left[i\kappa\sin^2\phi\frac{u^R(h, \omega)}{v^R(0, \omega)} + \frac{1}{v^R(0, \omega)}\left(\frac{\partial v^R}{\partial z}\right)_{z=h}\right]. \qquad (2.9)$$

In general, if the fault plane is vertical and the motion dip or strike slip, the shape of the Rayleigh wave spectrum is the same for all azimuths, but for all other orientations, the shape will change with ϕ as well as the magnitude.

One of the major characteristics of the spectrum is the zero which may occur because the expression in square brackets in equation (2.6) has a zero. The simplest

Table 1

Standard continental crust with sediment (*Kanamori* 1967)

	α	β	ρ	depth
1st layer	3·00 km s^{-1}	1·66 km s^{-1}	2·35 g cm^{-3}	2·0 km
2nd layer	6·10 km s^{-1}	3·50 km s^{-1}	2·70 g cm^{-3}	9·0 km
3rd layer	6·40 km s^{-1}	3·68 km s^{-1}	2·90 g cm^{-3}	9·0 km
4th layer	6·70 km s^{-1}	3·94 km s^{-1}	2·90 g cm^{-3}	18·0 km
Half Space	8·15 km s^{-1}	4·75 km s^{-1}	3·30 g cm^{-3}	

case to examine is that of vertical strike slip. If the half space is uniform, the displacement component u^R has magnitude given by

$$|u^R(z, \omega)| = \kappa^{-1} B\,|\exp(-\kappa\eta_\alpha z) - (1 - c_R^2/2\beta^2)\exp(-\kappa\eta_\beta z)|, \qquad (2.10)$$

where

$$\eta_\alpha = (1 - c_R^2/\alpha^2)^{\frac{1}{2}}, \qquad \eta_\beta = (1 - c_R^2/\beta^2)^{\frac{1}{2}}$$

$$c_R = \omega/\kappa, \qquad B \text{ is a constant.}$$

Therefore $u^R(h, \omega)$ has a node at the frequency which satisfies

$$h\omega/c_R = -[\log(1 - c_R^2/2\beta^2)]/(\eta_\alpha - \eta_\beta). \qquad (2.11)$$

This has a solution (real and positive ω) for all h. Hence, if the source is a vertical strike slip, the zero in the Rayleigh wave spectrum gives an exact indication of the depth. Fig. 1 shows the amplitude of $\kappa u^R(h, \omega)$ as a function of $\omega h/c_R$; i.e. as a function of depth or of frequency. The elastic parameters used were those of a Poisson solid ($\lambda = \mu$). Considered as a frequency spectrum, this needs to be multiplied by

$$|\bar{Q}(\omega)\,\bar{u}_z^{q2}(r, 0, \omega)\sin 2\phi/v^R(0, \omega)|$$

to give the total Rayleigh wave spectrum for a vertical strike slip fault.

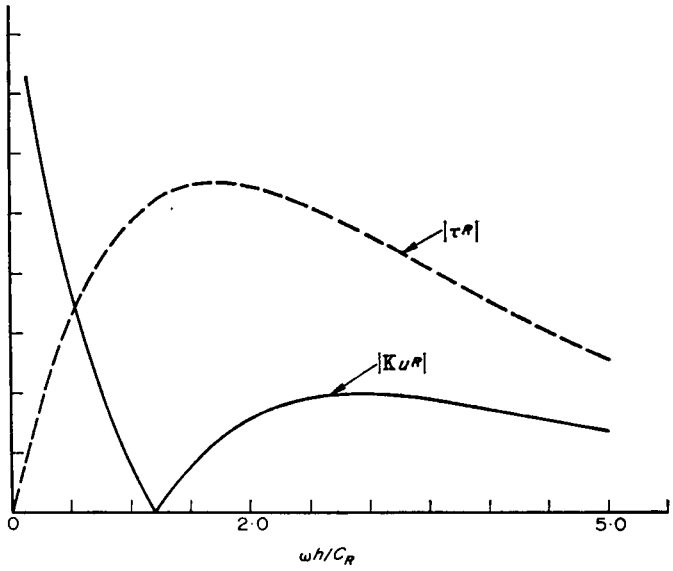

FIG. 1. The factors in the Rayleigh wave spectrum involving source mechanism and depth for a vertical strike-slip $|\kappa u^R|$ and a vertical dip-slip $|\tau^R|$ fault in a half space with $\lambda = \mu$.

The magnitude of τ^R is given by

$$|\tau^R(z, \omega)| = 2\eta_\alpha \mu B \,|\exp(-\kappa\eta_\alpha z) - \exp(-\kappa\eta_\beta z)|, \qquad (2.12)$$

which has a zero at the surface $z = 0$ only (see Fig. 1). So there is no zero from this cause in the Rayleigh wave spectrum of a vertical dip slip source.

The expression on the right-hand side of equation (2.9) for the 45° dip slip gives a factor with amplitude

$$\left|(1+\sin^2\phi)[\exp(-\kappa\eta_\alpha h) - (1 - c_R{}^2/2\beta^2)\exp(-\kappa\eta_\beta h)] - \frac{c_R{}^2}{\alpha^2}\exp(-\kappa\eta_\alpha h)\right|. \qquad (2.13)$$

Fig. 2 shows this expression as a function of $\omega h/c_R$ for several azimuths. It has a zero at values of $\omega h/c_R$ which vary with azimuth. This variation is shown in Fig. 3.

It is clear from Figs 1 and 2 that the effect of source mechanism on the Rayleigh wave spectrum is quite striking. The principle characteristic of the graphs shown is the zero corresponding to a node in a certain combination of the displacements in a free moving Rayleigh wave. This characteristic is repeated in the corresponding expressions calculated for a layered half-space. For certain structures it is found that $\tau^R(z, \omega)$ also has a zero at $z > 0$. Such spectral 'holes' are in fact observed (see Marshall & Burton 1971, in preparation).

Fig. 4 shows $\tau^R(z, \omega)$ and $u^R(z, \omega)$ as functions of z calculated for the structure given in Table 1 and at approximately 20-s period. Both curves are similar to those corresponding to a uniform half-space except that, in this case, τ^R has a zero at fairly shallow depth. (There are also discontinuities in slope at layer boundaries.)

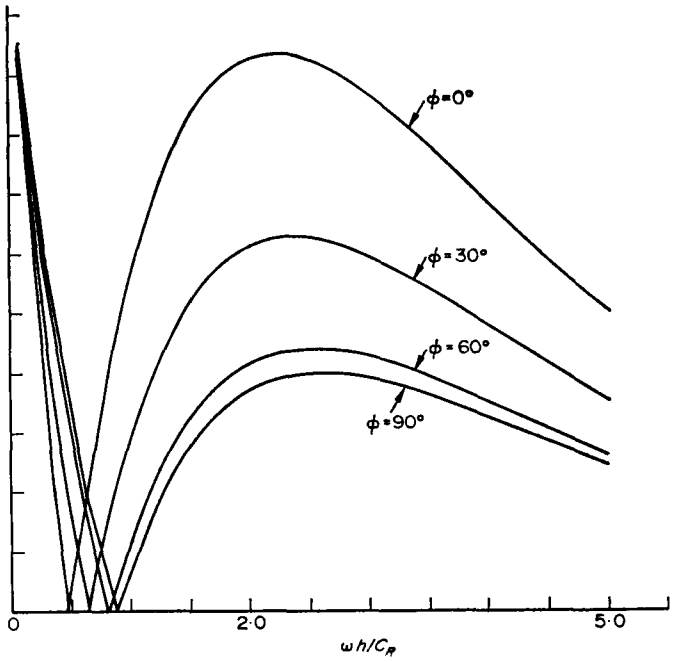

FIG. 2. The factor in the Rayleigh wave spectrum involving source mechanism and depth for a dip-slip on a 45° slope (equation (2·13) with $\lambda = \mu$) for various values of the azimuth ϕ ($\phi = 0$ is the direction of strike).

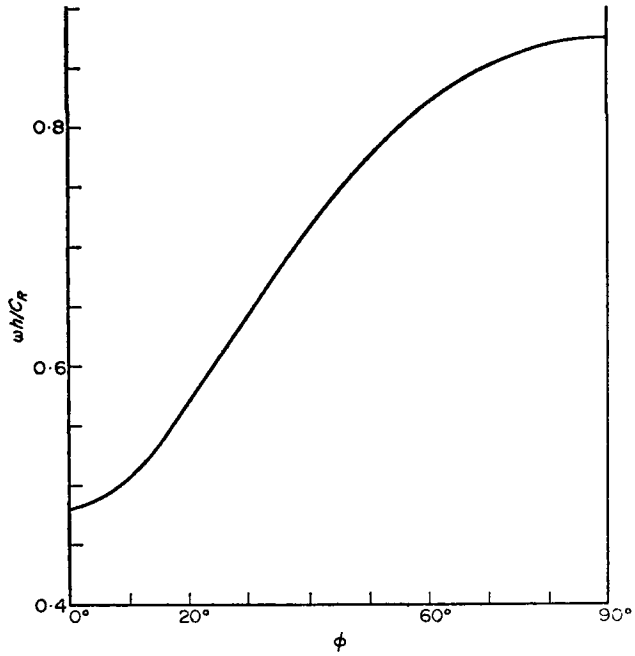

FIG. 3. The variation of the Rayleigh wave spectral zero, for a dip-slip source with 45° angle of dip, with azimuth ϕ.

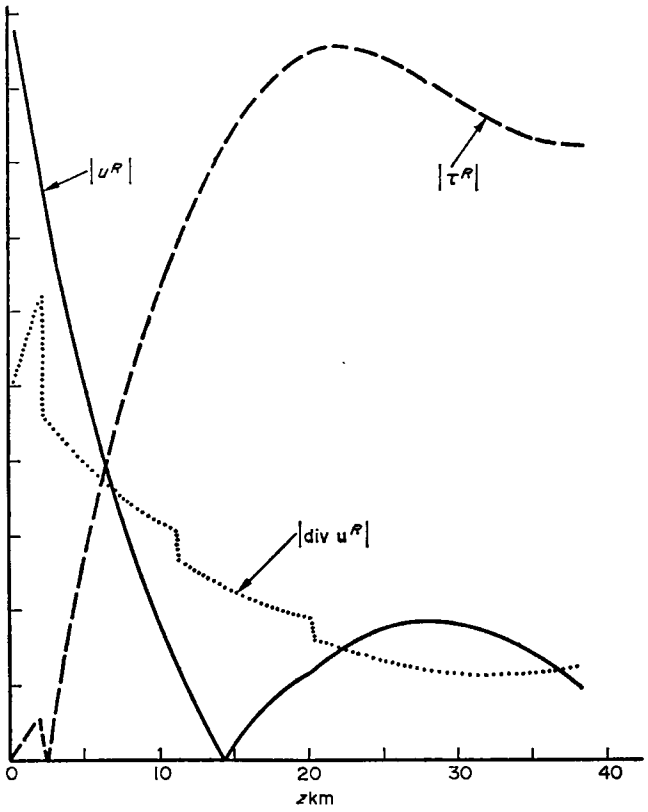

FIG. 4. The horizontal displacement u^R, the divergence of the displacement div u^R, and the shear stress on a horizontal plane τ^R in a Rayleigh wave, travelling in the crust given in Table 1, as functions of depth z. (Period 19·7 seconds.)

Both u^R and τ^R are no longer simply functions of $\omega h/c_R$ but are functions of two variables ω and h. In the case of a uniform half-space, the period at which the zero occurs depends linearly on the source depth. In this case the relationship is non-linear and is shown for u^R and τ^R in Fig. 5.

From the curve corresponding to u^R in Fig. 5(a) one can see that, for a vertical strike slip fault in a crust of the structure given in Table 1 at a depth of 15 km, measurement of M_s based on the amplitude of 20-s period Rayleigh waves are almost certain

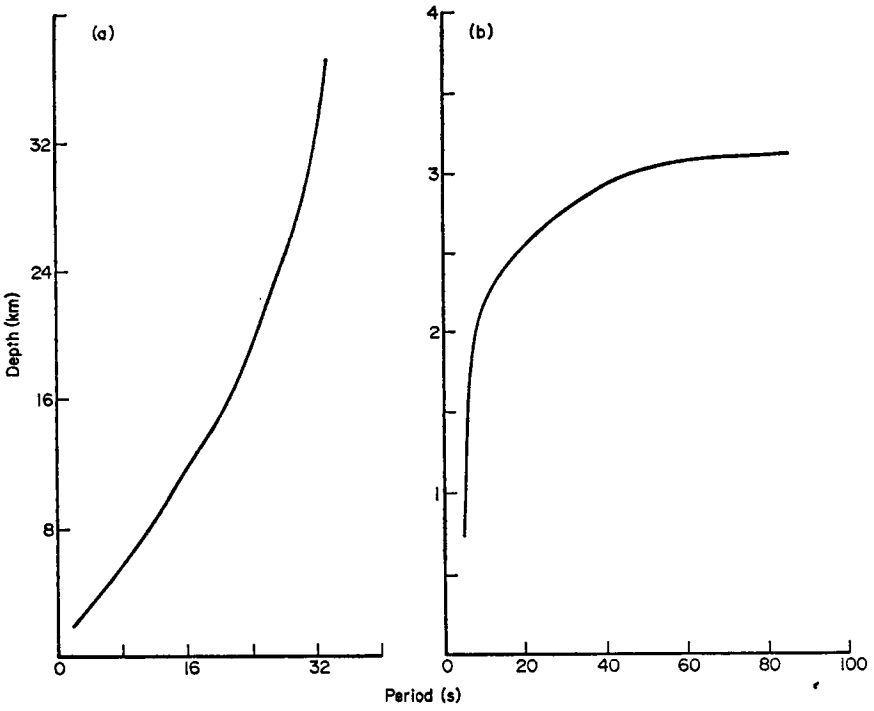

FIG. 5. The relationship between depth and period in the zeros of (a) $u^R(z, \omega)$, and (b) $\tau^R(z, \omega)$, both calculated for the crust in Table 1.

to give misleading results, as the measurements will be made exactly where the spectrum has a hole. The curve for τ^R indicates that a vertical dip slip fault in such a crust at 2–3 km depth will give rise to Rayleigh waves with anomolously low magnitudes in general.

The effect of source mechanism and depth on the Rayleigh wave spectrum is best seen in the graphs of

$$\left|\frac{\kappa u^R(h, \omega)}{v^R(0, \omega)}\right| \quad \text{and} \quad \left|\frac{\tau^R(h, \omega)}{\mu_m v^R(0, \omega)}\right|$$

as functions of period. Fig. 6 shows such curves for a depth of 2 km. The parameters have been specifically chosen such that τ^R has a zero. The effect of crustal structure can be seen by comparing these with the corresponding curves for a half space (Fig. 1).

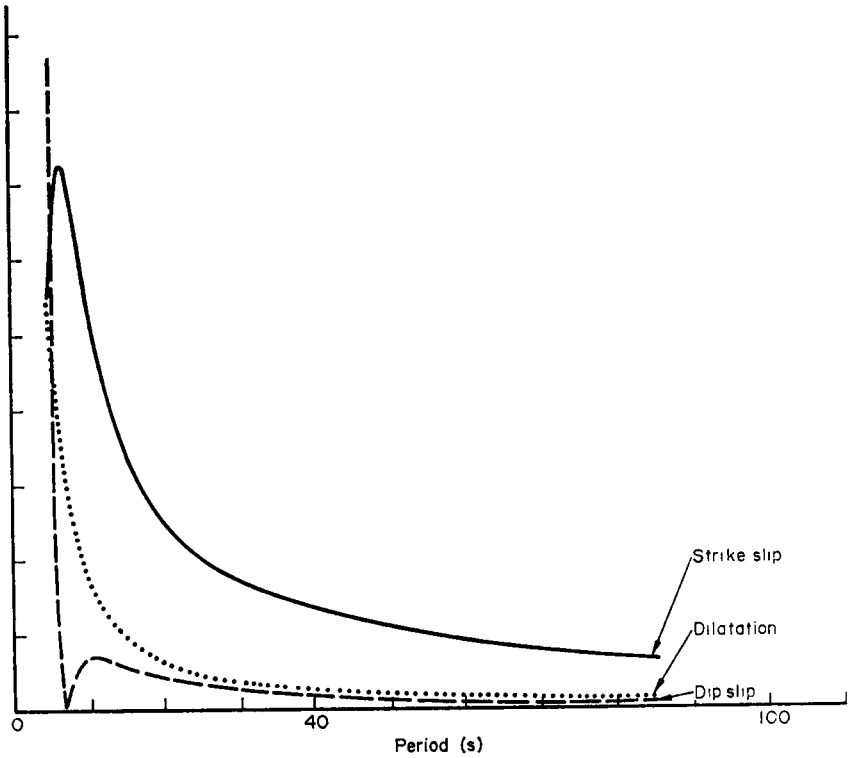

FIG. 6. The factors in the Rayleigh wave spectrum involving source mechanism and depth as functions of period for a vertical strike slip $\left|\frac{2\kappa u^R(h,\omega)}{v^R(o,\omega)}\right|$, vertical dip slip $\left|\frac{\tau^R(h,\omega)}{\mu_m v^R(o,\omega)}\right|$ and dilation $\left|\frac{\text{div } \mathbf{u}^R(h,\omega)}{2v^R(o,\omega)}\right|$ fault at a depth of 2 km in the crust given in Table 1.

3. Rayleigh waves from a dilatation source

If we take the force generating the displacements $\mathbf{u}^{1q}$ to be a point dilatation of magnitude $Q'(t)$ acting at depth h' we get, in place of equation (2.3),

$$\bar{u}_z^{1q}(r,\phi,0,\omega) = \bar{Q}'(\omega)\frac{\partial}{\partial x_j}\bar{u}_j^{2q}(0,\phi+\pi,h',\omega)$$

$$= \bar{Q}'(\omega)\bar{u}_z^{2q}(r,0,\omega)\left[\frac{\left(\frac{\partial v^R}{\partial z}\right)_{z=h'} - i\kappa u^R(h',\omega)}{v^R(0,\omega)}\right]. \qquad (3.1)$$

In a uniform half space

$$\frac{\partial v^R}{\partial z} - i\kappa u^R = -\frac{\omega^2}{\alpha^2}B\exp(-\kappa\eta_\alpha z). \qquad (3.2)$$

This is of course independent of azimuth and is clearly not zero for any value of z. The expression

$$\frac{\partial v^R}{\partial z} - i\kappa u^R = \operatorname{div} \mathbf{u}^R \tag{3.3}$$

is drawn in Figs 4 and 6 as function of depth and period for the layered structure given in Table 1. It is clear that although the divergence is a discontinuous function of z (at layer boundaries), dilatation sources give a fairly smooth spectrum.

We can compare the relative excitation of Rayleigh waves by double couple and dilatation sources acting in the same region of the Earth by forming the magnitude of the ratio of expressions (2.6) and (3.1):

$$\chi^R = \left|\frac{\bar{Q}(\omega)}{\bar{Q}'(\omega)}\right| \Big| i\kappa(q_0 - q_2)\, u^R(h,\omega) + i\kappa q_1\, v^R(h,\omega) + 2q_0 \left(\frac{\partial v^R}{\partial z}\right)_{z=h} - q_1 \left(\frac{\partial u^R}{\partial z}\right)_{z=h} \Big| |(\operatorname{div} \mathbf{u}^R)_{z=h}|^{-1}. \tag{3.4}$$

In taking this ratio, all complex transmission effects which may be allowed for by a linear transfer function have cancelled out. So the expression above may be expected to give a good approximation to the value of χ^R calculated from data.

This means that, if the structure in the neighbourhood of the sources is known, with data from an explosive source of known yield and depth, the mechanism and depth of a nearby fault slip may be found fairly accurately. Alternatively, if the mechanism and depth of a fault slip in the area is known, the nature and depth of a nearby explosion may be found. (One might investigate the relationship of aftershocks to the main shock in a similar way.) This is subject to the proviso, as before, that the sources are small enough to be considered as acting at a point.

If the half space is uniform, we get

$$\chi^R = \left|\frac{\bar{Q}(\omega)}{\bar{Q}'(\omega)}\right| \frac{\alpha^2}{c_R^2} \Big| \left\{ \left[3(1 - c_R^2/2\beta^2) E - 3 + \frac{2c_R^2}{\alpha^2} \right] q_0 + 2i\eta_\alpha (1-E) q_1 + [1 - (1 - c_R^2/2\beta^2) E] q_2 \right\} \exp[\kappa\eta_\alpha(h'-h)] \Big|, \tag{3.5}$$

where $E = \exp[\kappa h(\eta_\alpha - \eta_\beta)]$. (This expression compares accurately with Haskell 1963.)

Fig. 7 shows expression (3.5) evaluated for each type of the three basic faults described in Section 2 and for $h = h'$ and $h = 10h'$ When the two source depths are equal the exponential factor E dominates at high frequencies or large source depths (large $\omega h/c_R$) and χ^R becomes exponentially large. This is because, as the depth of source increases, the Rayleigh magnitudes for the faults go down as $\exp(-\kappa h\eta_\beta)$, but those of the dilatation source as $\exp(-\kappa h\eta_\alpha)$. So the absolute magnitudes of the Rayleigh waves go down but the relative excitation by the fault to that by the dilatation increases.

The preferential excitation of Rayleigh waves by earthquakes to that by explosions is a useful technique for discrimination. Given the depth of source then, it is clear that in this case one would look at high frequencies to discriminate between the two types of source.

When the fault is at greater depths than the dilatation, the character of the curves changes. In this case the factor $\exp[\kappa\eta_\alpha(h'-h)]$ dominates and χ^R becomes exponentially small at high frequencies. It has a peak around $(\omega h/c_R) = 2$ to 3 in the

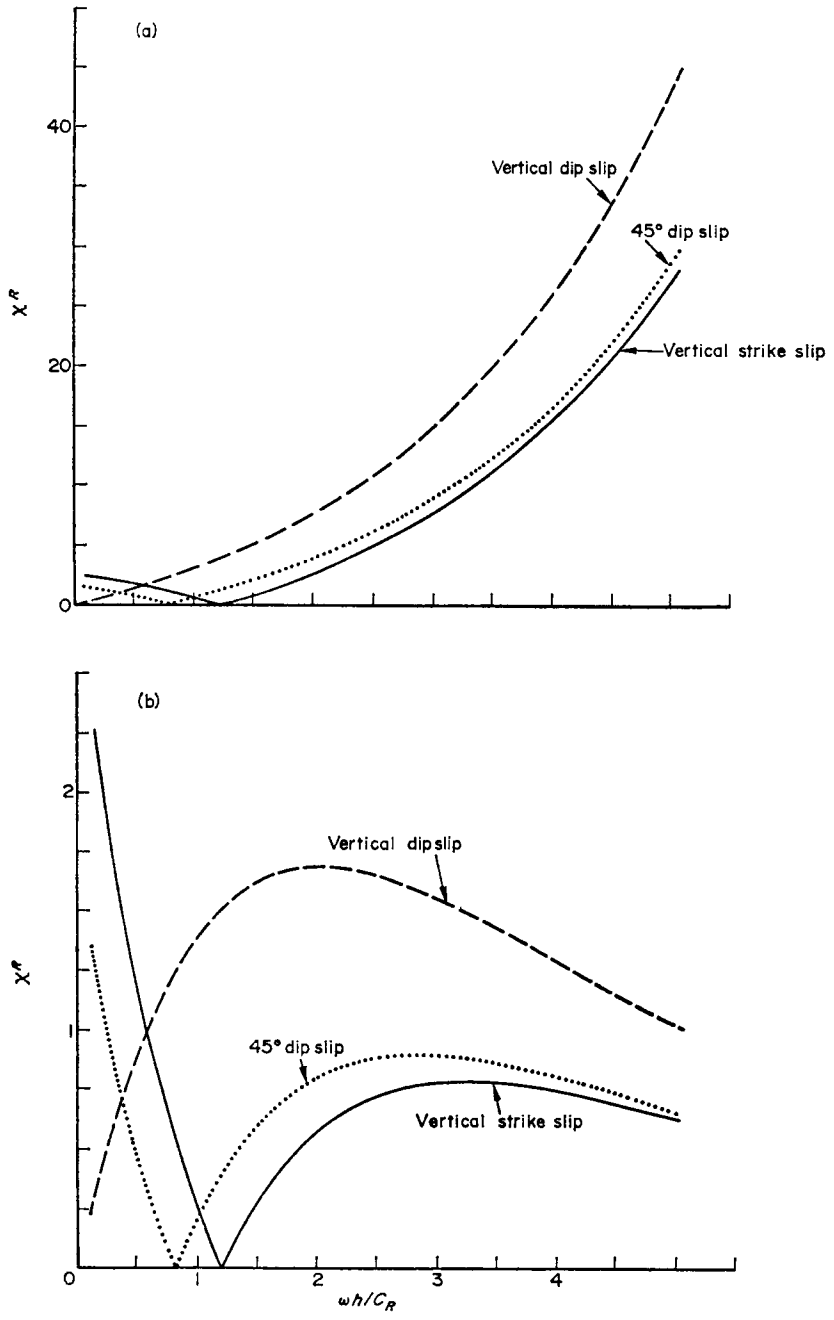

FIG. 7. The ratio χ^R of Rayleigh wave generation by double couple faults to that by a dilatation fault in a half space with $\lambda = \mu$ (equation (3·5) with $\bar{Q}(\omega)/\bar{Q}'(\omega) = 2$ for vertical strike-slip and 1 otherwise) with (a) $h = h'$, and (b) $h = 10h'$. ($\phi = 60°$ throughout).

examples shown. For a depth of 10 km, this corresponds to a Rayleigh wavelength of 20–30 km. So one may expect the discrimination method to work best at these wavelengths. However, the method also depends on the relative generation of body waves, so this is only a tentative conclusion.

Since $\operatorname{div} \mathbf{u}^R$ is a fairly smooth function, the major characteristics of the curves in Fig. 7 are those of the spectra of the respective fault types. The spectral holes are clearly in evidence in the cases of vertical strike slip and of dip slip on a 45° slope.

4. Love waves from a double-couple source

If we substitute into the reciprocal theorem A22

$$\left.\begin{aligned} f_1{}^2 &= -\delta(x_1 - r_1\cos\phi_1)\,\delta(x_2 - r_1\sin\phi_1)\,\delta(x_3)\,\delta(t)\sin\phi_1 \\ f_2{}^2 &= \delta(x_1 - r_1\cos\phi_1)\,\delta(x_2 - r_1\sin\phi_1)\,\delta(x_3)\,\delta(t)\cos\phi_1 \\ f_3{}^2 &= 0, \end{aligned}\right\} \tag{4.1}$$

(i.e. a unit point force at the surface at distance r_1 and azimuth ϕ_1, acting in the ϕ-direction) we get, instead of equation (2.3),

$$\bar{u}_\phi{}^{1q}(r_1, \phi_1, 0, \omega) = 2\bar{Q}(\omega)\,\bar{\varepsilon}_{fn}^{2q}(\phi_1 + \pi, h, \omega), \tag{4.2}$$

where the shear strain ε_{fn}^{2q} is that due to the Love waves emitted by the source (4.1) at azimuth $\phi_1 + \pi$.

Since the Love waves at large distances are approximately plane and of a standard form, we may write

$$\left.\begin{aligned} \bar{u}_1{}^{2q}(0, \phi_1 + \pi, z, \omega) &= C'\,u^L(z, \omega)\sin\phi_1 \\ \bar{u}_2{}^{2q}(0, \phi_1 + \pi, z, \omega) &= -C'\,u^L(z, \omega)\cos\phi_1 \\ \bar{u}_3{}^{2q}(0, \phi_1 + \pi, z, \omega) &= 0, \end{aligned}\right\} \tag{4.3}$$

where C' is a constant and u^L contains a factor $\exp[i\kappa^L(x_1\cos\phi_1 + x_2\cos\phi_2)]$ (κ^L is the Love wave number). Substituting into the expression for $\bar{\varepsilon}_{fn}^{2q}$ we obtain

$$\bar{\varepsilon}_{fn}^{2q}(\phi_1 + \pi, h, \omega) = \tfrac{1}{2}C'\left[q_1'\left(\frac{\partial u^L}{\partial z}\right)_{z=h} + q_2'\,i\kappa^L\,u^L(h, \omega)\right], \tag{4.4}$$

where

$$q_1' = (f_1 n_3 + f_3 n_1)\sin\phi_1 - (f_2 n_3 + f_3 n_2)\cos\phi_1$$

$$q_2' = (f_1 n_1 - f_2 n_2)\sin 2\phi_1 - (f_1 n_2 + f_2 n_1)\cos 2\phi_1.$$

Hence equation (4.2) becomes

$$\bar{u}_\phi{}^q(r, \phi, 0, \omega) = \bar{Q}(\omega)\,\bar{u}_\phi{}^{3q}(r, 0, \omega)\left[\frac{q_1'}{u^L(0, \omega)}\left(\frac{\partial u^L}{\partial z}\right)_{z=h} + q_2'\,i\kappa^L\,\frac{u^L(h, \omega)}{u^L(0, \omega)}\right], \tag{4.5}$$

where we have dropped the superscripts and subscripts 1; $\bar{u}_\phi{}^{3q}(r, z, \omega)$ is the Love wave displacement at a distance r and azimuth $\pi/2$ from a unit point force acting at the origin in the direction $\phi = 0$.

For a vertical dip slip source,

$$\bar{u}_\phi{}^q(r, \phi, 0, \omega) = -\bar{Q}(\omega)\,\bar{u}_\phi{}^{3q}(r, 0, \omega)\,\frac{\cos\phi}{u^L(0, \omega)}\left(\frac{\partial u^L}{\partial z}\right)_{z=h}$$

$$= -\bar{Q}(\omega)\,\bar{u}_\phi{}^{3q}(r, 0, \omega)\,\frac{\cos\phi}{\mu_m}\left[\frac{\tau^L(h, \omega)}{u^L(0, \omega)}\right], \tag{4.6}$$

where τ^L is the shear stress on a horizontal plane in the standard Love wave.

For vertical strike slip

$$\bar{u}_\phi{}^q(r, \phi, 0, \omega) = -\bar{Q}(\omega)\,\bar{u}_\phi{}^{3q}(r, 0, \omega)\cos 2\phi\left[\frac{i\kappa^L u^L(h, \omega)}{u^L(0, \omega)}\right]. \tag{4.7}$$

Finally, for dip slip on a plane with angle of dip 45°,

$$\bar{u}_\phi{}^q(r, \phi, 0, \omega) = -\bar{Q}(\omega)\,\bar{u}_\phi{}^{3q}(r, 0, \omega)\sin 2\phi\left[\frac{i\kappa^L u^L(h, \omega)}{2u^L(0, \omega)}\right]. \tag{4.8}$$

Fig. 8 shows $\kappa^L u^L(z, \omega)$ and $\tau^L(z, \omega)$ as functions of depth and period for a uniform half space with a single uniform layer above (as in Table 2).

It can be shown (Hudson 1962) that, whatever the variation of elastic properties

Table 2

Crust with a single layer on a half space

	β	depth
1st layer	3·52 km s^{-1}	38 km
Half space	4·70 km s^{-1}	

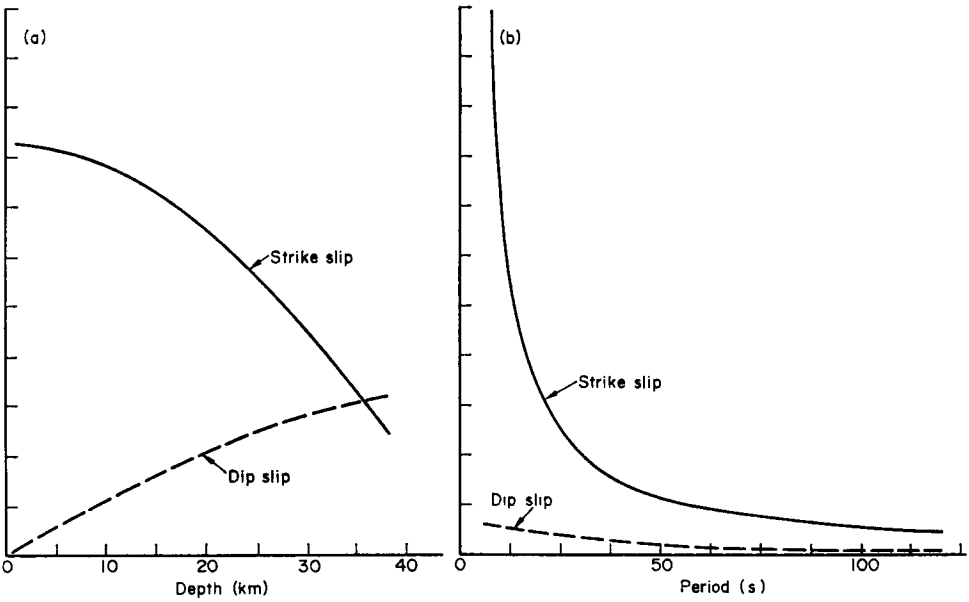

FIG. 8. The factors in the Love wave spectrum involving source mechanism and depth for a vertical strike slip $\left|\frac{\kappa^L u^L(h, \omega)}{u^L(o, \omega)}\right|$ and a vertical dip slip $\left|\frac{\tau^L(h, \omega)}{\mu u^L(o, \omega)}\right|$ fault in a half space with a single layer above; (a) As functions of depth at 20-s. period; and (b) As functions of period at a depth 10 km.

with depth, u^L will not go to zero in the fundamental Love wave. So the vertical strike slip fault will not have a zero from this cause in its Love wave spectrum. In Fig. 8 τ^L does not have a zero either, but it is conceivable that it might have, if the structure of the medium were different.

Conclusions

The reciprocity theorem gives a method by which the effects of source mechanism and depth on the surface wave spectra of the resulting radiation can be calculated, separate from the effect of the transmission path. It also leads to an explanation of certain holes appearing in surface wave spectra, to a possible method of checking fault plane solutions together with estimates of depth, and to a certain insight into the problems of calculating earthquake magnitudes using M_s. It is clear that a depth correction term of the type used in the formula for M_s proposed by Båth (1952) is inadequate, since the variation of surface wave magnitudes with depth of source is more complex than simple exponential-type decay, and depends on source type and orientation.

Acknowledgment

Mr V. K. Kembhavi has been supported during the period of this research by a grant from the National Environment Research Council.

A. Douglas;
U.K.A.E.A. Blacknest,
Brimpton,
Reading,
Berkshire

J. A. Hudson and, V. K. Kembhavi,
Department of Applied
Mathematics and Theoretical Physics,
Silver Street,
Cambridge

References

Båth, M., 1952. *Trans. Am. geophys. Un.*, **33.**
Burridge, R., Lapwood, E. R. & Knopoff, L., 1964. *Bull. seism. Soc. Am.*, **54,** 1889–1913.
Graffi, D., 1947. *Memorie della Accademia Scienze, Bologna*, Ser. 10, **4,** 103–109.
Gupta, I. N., 1966. *Bull. seism. Soc. Am.*, **56,** 925–936.
Haskell, N. A., 1963. *Bull. seism. Soc. Am.*, **53,** 619–642.
Hudson, J. A., 1962. *Geophys. J. R. astr. Soc.*, **6,** 131–147.
Hudson, J. A., 1969a. *Geophys. J. R. astr. Soc.*, **18,** 233–249.
Hudson, J. A., 1969b. *Geophys. J. R. astr. Soc.*, **18,** 353–370.
Kanamori, H., 1967. *Bull. Earth. Res. Inst. Tokyo*, 45.
Marshall, P. D. & Burton, P. W., 1971. *Geophys. J. R. astr. Soc.* (in preparation).
Wheeler, L. T. & Sternberg, E., 1968. *Arch. Rat. Mech. Anal.* **31,** 51–90.

Appendix

Reciprocal theorem for surface waves

Consider an elastic half space whose properties vary with depth only. A displacement field $\mathbf{u}(\mathbf{x}, t)$ and corresponding stress $\boldsymbol{\tau}(\mathbf{x}, t)$ satisfy the elastodynamic equations of motion

$$\rho \frac{\partial^2 u_i}{\partial t^2} = \frac{\partial \tau_{ij}}{\partial x_j} + \rho f_i, \tag{A1}$$

(where $\mathbf{f}(\mathbf{x}, t)$ is the body force per unit mass) and the linear stress–strain relations

$$\tau_{ij} = \lambda\delta_{ij}\frac{\partial u_k}{\partial x_k} + \mu\left(\frac{\partial u_i}{\partial x_j} + \frac{\partial u_j}{\partial x_i}\right). \tag{A2}$$

If the displacements and stresses are transformed by

$$\left.\begin{aligned} U_r^c(k, n, z, \omega) &= -\frac{1}{\pi}\int_{-\infty}^{\infty}\exp(-i\omega t)\,dt\int_{-\pi}^{\pi}\cos n\phi\,d\phi\int_0^{\infty}J_n(kr) \\ &\qquad\times\left\{\frac{\partial}{\partial r}(ru_r)+\frac{\partial u_\phi}{\partial\phi}\right\}\frac{dr}{k} \qquad n = 1, 2, \ldots \\ U_r^c(k, 0, z, \omega) &= -\frac{1}{2\pi}\int_{-\infty}^{\infty}\exp(-i\omega t)\,dt\int_{-\pi}^{\pi}d\phi\int_0^{\infty}J_0(kr) \\ &\qquad\times\left\{\frac{\partial}{\partial r}(ru_r)+\frac{\partial u_\phi}{\partial\phi}\right\}\frac{dr}{k}, \end{aligned}\right\} \tag{A3}$$

etc. (see Hudson 1969a), where r, ϕ, z are cylindrical polar co-ordinates such that the half space is defined by $z \geqslant 0$ and u_r, u_ϕ, u_z are the corresponding co-ordinates of $\mathbf{u}$, then the vectors

$$\mathbf{B}^\sigma(k, n, z, \omega) = \begin{pmatrix} U_r^\sigma \\ U_z^\sigma \\ T_z^\sigma \\ T_r^\sigma \end{pmatrix} \quad \text{and} \quad \mathbf{b}^\sigma = \begin{pmatrix} U_\phi^\sigma \\ T_\phi^\sigma \end{pmatrix} \tag{A4}$$

satisfy

$$\frac{\partial}{\partial z}\mathbf{B}^\sigma = \mathbf{N}\mathbf{B}^\sigma - \mathbf{Z}^\sigma, \qquad \frac{\partial}{\partial z}\mathbf{b}^\sigma = \mathbf{n}\mathbf{b}^\sigma - \mathbf{z}^\sigma \tag{A5}$$

by virtue of equations (A1) and (A2) (σ stands for either c or s; U_r^s etc. representing components transformed using $\sin n\phi$ instead of $\cos n\phi$). The square matrices $\mathbf{N}$, $\mathbf{n}$ depend on λ, μ, ρ, k only, and

$$\mathbf{Z}^\sigma(k, n, z, \omega) = \begin{pmatrix} 0 \\ 0 \\ Z_z^\sigma \\ Z_r^\sigma \end{pmatrix} \qquad \mathbf{z}^\sigma = \begin{pmatrix} 0 \\ Z_\phi^\sigma \end{pmatrix}, \tag{A6}$$

where

$$\left.\begin{aligned} Z_r^c(k, n, z, \omega) &= -\frac{\rho}{\omega^2\pi}\int_{-\infty}^{\infty}\exp(-i\omega t)\,dt\int_{-\pi}^{\pi}\cos n\phi\,d\phi\int_0^{\infty}J_n(kr) \\ &\qquad\times\left\{\frac{\partial}{\partial r}(rf_r)+\frac{\partial f_\phi}{\partial\phi}\right\}\frac{dr}{k} \qquad n = 1, 2, \ldots \\ Z_r^c(k, 0, z, \omega) &= -\frac{\rho}{2\omega^2\pi}\int_{-\infty}^{\infty}\exp(-i\omega t)\,dt\int_{-\pi}^{\pi}d\phi\int_0^{\infty}J_0(kr) \\ &\qquad\times\left\{\frac{\partial}{\partial r}(rf_r)+\frac{\partial f_\phi}{\partial\phi}\right\}\frac{dr}{k}, \end{aligned}\right\} \tag{A7}$$

etc. (other components being defined in a similar manner to U_z^σ, U_ϕ^σ with the extra factor ρ/ω^2).

The first of equations (A5) applied to two vectors $\mathbf{B}^{1\sigma}$ and $\mathbf{B}^{2\gamma}$ ($\gamma = s$ or c) corresponding to two different displacement fields, leads to

$$\frac{\partial}{\partial z}\mathscr{F}(z) = U_r^{2\gamma} Z_r^{1\sigma} - U_r^{1\sigma} Z_r^{2\gamma} + \frac{1}{k^2} U_z^{2\gamma} Z_z^{1\sigma} - \frac{1}{k^2} U_z^{1\sigma} Z_z^{2\gamma}, \tag{A8}$$

where

$$\mathscr{F}(z) = U_r^{1\sigma} T_r^{2\gamma} - U_r^{2\gamma} T_r^{1\sigma} + \frac{1}{k^2} U_z^{1\sigma} T_z^{2\gamma} - \frac{1}{k^2} U_z^{2\gamma} T_z^{1\sigma}. \tag{A9}$$

If the upper surface is stress free in both systems, $\mathscr{F}(0) = 0$. If also the half space is uniform for large enough z and the regions of non-zero body force are bounded, the displacements for large z correspond to outgoing waves in a uniform medium. It can be shown (*cf.* Hudson 1969b) that this implies that $\mathscr{F}(z) = 0$ for sufficiently large z.

Integrating equation (A8) over z we get

$$\int_0^\infty \left(U_r^{2\gamma} Z_r^{1\sigma} + \frac{1}{k^2} U_z^{2\gamma} Z_z^{1\sigma}\right) dz = \int_0^\infty \left(U_r^{1\sigma} Z_r^{2\gamma} + \frac{1}{k^2} U_z^{1\sigma} Z_z^{2\gamma}\right) dz. \tag{A10}$$

Similarly, from the second of equations (A5),

$$\int_0^\infty U_\phi^{2\gamma} Z_\phi^{1\sigma} dz = \int_0^\infty U_\phi^{1\sigma} Z_\phi^{2\gamma} dz. \tag{A11}$$

It follows from the method of Hudson (1969b) that the far field displacements in the Rayleigh waves generated by either system 1 or 2 are given by

$$\bar{u}_r^{jq}(r, \phi, z, \omega) = A\kappa \sum_{n=0}^{\infty} \left\{\lim_{k\to\kappa} [F(k, \omega)\, U_r^{jc}(k, n, z, \omega_j)] \cos n\phi + \lim_{k\to\kappa} [F(k, \omega)\, U_r^{js}(k, n, z, \omega)] \sin n\phi\right\} \exp(in\pi/2), \tag{A12}$$

$j = 1, 2$, and the bar denotes the Fourier transform in time.

Similarly

$$\bar{u}_z^{jq}(r, \phi, z, \omega) = Ai \sum_{n=0}^{\infty} \left\{\lim_{k\to\kappa} [FU_z^{1c}] \cos n\phi + \lim_{k\to\kappa} [FU_z^{1s}] \sin n\phi\right\} \exp(in\pi/2). \tag{A13}$$

$F(k, \omega)$ is the characteristic function for Rayleigh waves with root $k = \kappa$ corresponding to the fundamental mode, and

$$A = -\left(\frac{2\pi}{|\kappa| r}\right)^{\frac{1}{2}} \exp[-i\kappa r \pm i\pi/4]/F'(\kappa, \omega); \tag{A14}$$

$F' = \partial F/\partial k$ and the $\pm$ sign depends on $\omega \gtrless 0$. (The sum over n is finite in most applications of this theory so that there are no convergence problems.)

From equation (A10) we now get, using (A12) and (A13),

$$\int_0^\infty \{i\kappa \bar{u}_r^{2q}(r, \phi_2, z, \omega)\, S^1(Z_r^1) + \bar{u}_z^{2q}(r, \phi_2, z, \omega)\, S^1(Z_z^1)\} dz = \int_0^\infty \{i\kappa \bar{u}_r^{1q}(r, \phi_1, z, \omega)\, S^2(Z_r^2) + \bar{u}_z^{1q}(r, \phi_1, z, \omega)\, S^2(Z_z^2)\} dz, \tag{A15}$$

where

$$S^j(Z_l^j) = \sum_{n=0}^{\infty} \{Z_l^{jc}(\kappa, n, z, \omega) \cos n\phi_j + Z_l^{js}(\kappa, n, z, \omega) \sin n\phi_j\} \exp(in\pi/2),$$

$j = 1, 2$ and l represents r or z. (The integral over z is in fact finite since the integrand is zero for large enough z, so there is again no problem of convergence.)

By using the representation

$$2\pi i^n J_n(\kappa r) = \int_{-\pi}^{\pi} \exp(i\kappa r \cos\phi) \cos n\phi \, d\phi, \tag{A16}$$

it can be shown that

$$S^j(Z_r^j) = -\frac{\rho}{2\pi\omega^2 \kappa} \int_0^{\infty} r dr \int_{-\pi}^{\pi} d\phi \left\{ \frac{1}{r} \left[\frac{\partial r \bar{f}_r^j(r, \phi, z)}{\partial r} + \frac{\partial \bar{f}_\phi^j(r, \phi, z)}{\partial \phi} \right] \times \exp[i\kappa r \cos(\phi - \phi_j)] \right\} \tag{A17}$$

$$= \frac{i\rho}{2\pi\omega^2} \int_0^{\infty} r dr \int_{-\pi}^{\pi} d\phi \{[\bar{f}_r^j \cos(\phi - \phi_j) - \bar{f}_\phi^j \sin(\phi - \phi_j)] \times \exp[i\kappa r \cos(\phi - \phi_j)]\}$$

and

$$S^j(Z_z^j) = \frac{\rho\kappa}{2\pi\omega^2} \int_0^{\infty} r dr \int_{-\pi}^{\pi} d\phi \{\bar{f}_z^j(r, \phi, z) \exp[i\kappa r \cos(\phi - \phi_j)]\}, \tag{A18}$$

$j = 1, 2$.

The integrands of (A17) and (A18) are in the form of a component of $\mathbf{f}^j$ multiplied by a plane wave with wave number κ, moving in a direction making an angle $\phi_j + \pi$ with $\phi = 0$. This is exactly the form of a Rayleigh wave arriving from a source at a very large distance r in the opposite direction.

We may take $\phi_1 = \phi_2 + \pi$ without loss of generality as the orientation of the fault systems may be chosen arbitrarily; by substitution of (A17), (A18) into (A15) we get

$$\int_{V_1} \mathbf{u}^{2q}(r, \phi_1 + \pi, z, \omega) . \bar{\mathbf{f}}^1(r, \phi, z, \omega) \, dV = \int_{V_2} \mathbf{u}^{1q}(r, \phi_1, z, \omega) \, \mathbf{f}^2(r, \phi, z, \omega) \, dV, \tag{A19}$$

where $\mathbf{f}^1$, $\mathbf{f}^2$ represent force systems a large distance apart lying within the regions V_1, V_2 and $\mathbf{u}^{1q}$, $\mathbf{u}^{2q}$ represent the Rayleigh waves generated by each respectively; the two-body force systems may be thought to be connected by a line from 1 to 2 making an angle ϕ_1 with the plane $\phi = 0$.

The far field displacements in the Love waves generated by either system 1 or system 2 are given by

$$\bar{u}_\phi^{jq}(r, \phi, z, \omega) = A^L \kappa^L \sum_{n=0}^{\infty} \left\{ \lim_{k \to \kappa^L} [F_L(k, \omega) U_\phi^{jc}(k, n, z, \omega)] \sin n\phi - \lim_{k \to \kappa^L} [F_L(k, \omega) U_\phi^{js}(k, n, z, \omega)] \cos n\phi \right\} \exp(in\pi/2) \qquad j = 1, 2 \tag{A20}$$

where κ^L is the wave number, F_L the characteristic equation of Love waves, and A^L is the factor corresponding to A.

By applying this relation to equation (A11), we get

$$\int_0^\infty \bar{u}_\phi{}^{2q}(r, \phi_2, z, \omega)\, s'(Z_\phi{}')\, dz = \int_0^\infty \bar{u}_\phi{}^{2q}(r, \phi_1, z, \omega)\, s^2(Z_\phi{}^2)\, dz,$$

where

$$s^j(Z_\phi{}^j) = \sum_{n=0}^{\infty} \{Z_\phi{}^{jc}(\kappa, n, z, \omega) \sin n\phi_j - Z_\phi{}^{js}(\kappa, n, z, \omega) \cos n\phi_j\}$$

$$= \frac{\rho}{2\omega^2 \pi\kappa} \int_0^\infty r dr \int_{-\pi}^{\pi} d\phi \left\{ \frac{1}{r} \left(\frac{\partial \bar{f}_r{}^j}{\partial \phi} - \frac{\partial (r\bar{f}_\phi{}^j)}{\partial r} \right) \exp\left[i\kappa r \cos(\phi - \phi_j) \right] \right\}$$

$$= \frac{i\rho}{2\pi\omega^2} \int_0^\infty r dr \int_{-\pi}^{\pi} d\phi \left\{ [\bar{f}_r{}^j \sin(\phi - \phi_j) + \bar{f}_\phi{}^j \cos(\phi - \phi_j)] \exp\left[i\kappa r \cos(\phi - \phi_j) \right] \right\} \tag{A21}$$

Therefore we obtain as before

$$\int_{V_1} \mathbf{u}^{2q}(r, \phi_1 + \pi, z, \omega) . \bar{\mathbf{f}}^1(r, \phi, z, \omega)\, dV = \int_{V_2} \mathbf{u}^{1q}(r, \phi_1, z, \omega) . \bar{\mathbf{f}}^2(r, \phi, z, \omega)\, dV, \tag{A22}$$

and this equation now holds for both Rayleigh waves (equation (A19)) and Love waves. It is exactly of the form of the Fourier time transform of Graffi's (1947) result for the total displacement field.